

Photocatalytic Bacterial Inactivation Using Bi-doped TiO₂/Kaolinite Under Visible Light Irradiation

Anthoni B. Aritonang^{1,*}, Ajuk Sapar¹, Annisa Furqonita¹

¹ Department of Chemistry, FMIPA, University of Tanjungpura, Pontianak, Indonesia

*Corresponding author. Email: anthoni.b.aritonang@chemistry.untan.ac.id

ABSTRACT

Bismuth-doped TiO₂ immobilized on kaolinite (Bi-TiO₂-K) were prepared via sol-gel method, then calcined at 450°C using kaolinite as the matrix and Bi(NO₃)₃ as the Bi³⁺ cationic source. The obtained Bi-TiO₂-K photocatalyst were characterized using X-ray diffraction (XRD), infrared absorption spectroscopy, diffuse reflectance spectroscopy, energy-dispersive X-ray spectroscopy (EDX) and scanning electron microscopy (SEM). The photocatalytic activity of the Bi-TiO₂-K was investigated on the bacterial inactivation of *Escherichia coli* (EC) and *Staphylococcus aureus* (SA) in water solution under visible light irradiation. The photocatalytic activity test for inactivating EC and SA bacteria was determined at room temperature and pH 7. Under visible light irradiation for 180 min, the Bi-TiO₂-K photocatalyst have higher bacterial inactivation as compared to unmodified Bi-TiO₂ photocatalyst. After 180 min irradiation time was required to achieve bacterial reduction for an average bacterial inoculum size of 9.5×10^6 CFU mL⁻¹. Finally, Bi doped TiO₂-K could be an efficient photocatalyst for bacterial strain inactivation.

Keywords: Bi-TiO₂; photocatalytic; kaolinite; antibacterial inactivation, visible light.

1. INTRODUCTION

High population growth has resulted in higher demand for clean water, but its supply is increasingly limited. Microorganism pollutants for example bacteria and fungi are living in water can harm human health [1], [2]. Disinfection of microorganisms in water so far generally uses chlorination method. The chlorination method using chlorine gas to produce chloro-organic disinfection which is a side-product of the reaction of chlorine with natural organic matter. Chloro-organic disinfection is carcinogenic which can endanger human health [3]. Therefore, simple clean water treatment technology is required. Therefore, finding out an effective water treatment technology without harmful treatment by products is required. Therefore, it is necessary to find an effective water treatment technology, without harmful by-product.

The semiconductor-based such as titanium dioxide (TiO₂) has been widely as photocatalyst for the inactivation of harmful pathogens and for the degradation of organic compounds in wastewater [4]–[6]. Titanium dioxide has been reported to be one of the most promising photocatalysts, because of its good photocatalytic

activity, better efficiency, stability and low cost [7]. Although TiO₂ generally shows high activity for the photocatalytic oxidation of organic pollutants, there are two drawbacks limiting its photocatalytic application: its low use of the solar spectrum because of its large band gap of 3.2 eV (anatase phase crystalline), only a small UV fraction (4–5%) of the solar light can be utilized and its relatively high electron-hole recombination rate [8].

In the past few years, bismuth-based oxide mixtures have been of great interest to researchers of visible light-activated photocatalysts, such as Bi₂O₃, Bi₂WO₆, Bi₂Mo₃O₁₂. Several papers have reported that the narrowing of the Bi band gap is the contribution of the 6s orbital electron transition to the conduction band, so that the response to visible light is getting better in these metal oxides compound. The Bi³⁺ cation where it has an ionic radius of 0.74 Å almost the Ti⁴⁺ ion 0.68 Å may be substituted by Bi³⁺ cations and can decrease the band gap of TiO₂ and thereby extend its absorption into the visible light region [9].

The numerous methods have been reported in the literature related to the synthesis of Bi-doped TiO₂ nanoparticles to improve their photocatalytic activities.

Lopez et al. have been prepared of Bi³⁺-doped TiO₂ with a doping concentration up to 2 wt% by a sol-gel hydrothermal method [10]. The presence of Bi³⁺ in TiO₂ enhances the photocatalytic degradation of phenol in aqueous solution under UV-vis illumination. Mao [11] have been fabricated Bi-TiO₂ using a sol-gel method. The 5% of Bi-TiO₂ powder shows superior photodegradation for rhodamine B efficiency of 95.6% under UV-vis irradiation for 60 min [11]. Magesan et al have been successfully synthesized 4% Bi₂O₃-TiO₂ nanocomposites via sol-gel method using CTAB as templating agent [12]. The responsively to visible light was found to mainly originate from the doping process as a result of the formation of new Bi states in the form of Bi-O-Ti bonds and the reduction in the electron-hole recombination rate [13]. A major issue with TiO₂ in general is, its easily agglomerate over time to minimize their surface area, which reduces its photocatalytic activity. On the other hand, the TiO₂ nanoparticles are difficult to separate for reuse from solution. The adsorption ability of the TiO₂ is relatively small, which cause in low photocatalytic activity [14], [15]. One way to overcome this problem can be done by using an impregnation on solid material surface as matrix supporting.

The activated carbon is chosen broadly as the support to increase remarkably the photocatalytic activity of TiO₂ because of the high adsorption capability of the carbon particles [16]. Therefore, improving the adsorption ability of the photocatalysts may be an efficient way to enhance the photocatalytic activity. Candraboss et al. have been synthesis activated charcoal (AC) supported bismuth (Bi)-doped Titanium dioxide (TiO₂) nanocomposite by precipitation method [17]. The incorporation of Bi³⁺ into the TiO₂ matrix shifts the absorbance of TiO₂ to the visible region then the addition of high adsorption capacity activated charcoal to improve the efficiency of TiO₂.

Clays such as kaolinite are known to have a higher surface area with interlayers available have been used as a support material. They are easily separable after activity thus making them promising support for photocatalysis as well. [14]. In previous studies, it is known that the addition of kaolinite can prevent the formation of TiO₂ agglomerates in the solution [6]. In addition, kaolinite can inhibit photo electron-photo hole pair recombination rate which contributes to increasing its photocatalytic activity. Kaolinite capkala are natural clay minerals which are very abundant in Capkala village, Bengkayang region, including phyllosilicates has an adsorption capacity of 0.65 mg/g, potentially used as a supporting material catalyst. Kaolinite, whose layered structure alumina silicate (Al₂Si₂O₅(OH)₄) provides the possibility of retention of a variety of compounds to reduce the energy required for the activation of the semiconductor. The catalyst improvement via immobilization might also be due to the force field

between the support and the TiO₂ particles can inhibits the recombination of electron-hole pairs [18].

The main aim of this study was to develop a Bi-TiO₂-K to enhance its photocatalytic inactivation of EC and SA under visible light irradiation.

2. MATERIALS AND METHOD

2.1. Chemicals and materials

All the chemicals were of analytical grade and used as received. Titanium tetraisopropoxide {Ti(OC₃H₇)₄, 98% TTIP} and bismuth nitrate (Bi(NO₃)₃.5H₂O, Sigma-Aldrich 96%), were used as precursor of Ti⁴⁺ and Bi³⁺ for preparing TiO₂ and Bi doped-TiO₂ photocatalysts. Acetyl acetone (C₅H₈O₂, 97%), acetic acid (CH₃COOH, 98%), ethanol (C₂H₅OH, 97%) were purchase from Merck, sodium chloride (NaCl, Sail brand 96%) and nitric acid (HNO₃, Merck 96%), natural kaolinite was obtained from capkala village Bengkayang. Deionized distilled water was used for preparing all aqueous solutions. Nutrient broth (Merck), inoculum bacterial E. coli Thermo ATCC 25922, and S.aureus ATCC 25923 and yeast extract (Himedia).

2.2. Preparation of Pure Kaolinite

5.0 grams of Kaolinite was dissolved in 40 mL of HCl 6M, leave the solution overnight at room temperature (30°C) to form a precipitate. The precipitate was separated from the solution and washed using distilled water until free of Cl⁻ anions, then dried it in an oven at 120 °C and followed calcined at 500 °C for 2 hours to produce pure kaolinite.

2.3. Preparation of TiO₂ and Bi-doped TiO₂ Sol

Preparation of TiO₂ sol using 7.5 mL of TTIP and 26.5 mL of ethanol mixed with 2 mL of acetic acid, 2 mL of distilled water and 1 mL of acetylacetone in a reflux device. The mixture was stirred while being heated at 55 °C for 2 hours to form a TiO₂ sol. To obtain a Bi-doped-TiO₂ sol, a solution of Bi (NO₃)₃.5H₂O was added to the TiO₂ sol while stirring for 2 hours. Synthesis of Bi-doped TiO₂/Kaolinite The 0.5 g of pure kaolinite was added in 10 mL distilled water and stirred for 15 min for uniform dispersion. Then, 25 mL Bi-doped TiO₂ sol which contained of Bi³⁺ : TiO₂ ratio (1.0 % b/v) was stirred with the pure kaolinite dispersion for 4 h and followed aging for 12 h to form Bi doped-TiO₂/kaolinite gel. The Bi doped-TiO₂/kaolinite gel was rinsed with distilled water and dried at 80 °C for 4 h to form Bi doped-TiO₂/kaolinite amorphous. Afterwards, the amorphous content was calcined at 450 °C for 3 h to form Bi doped-TiO₂/kaolinite composite. Bi³⁺ cations doping, the TiO₂ crystal and anchored into the kaolinite surface have occurred simultaneously during calcination

treatment. The same procedure was carried out for TiO₂/kaolinite composite as a control. Thus, the composited obtained were used for the further characterization and photocatalytic activity test.

2.4. Characterization of TiO₂ and Bi doped-TiO₂/kaolinite

The crystal phase of the photocatalyst were determined using an X-ray diffractometer (XRD-Shimadzu-7000) which was operated at 40 KV and 30 mA with Cu-K α 1 as radiation source of wavelength 1.54060 Å in the range scanning 20–80° (2 θ). The average crystallite size of sample was calculate using Sherrer formula [19–21]: $D = k \lambda / (\Delta \cos \theta)$, where $k = 0.94$; $\lambda = 1.54060 \text{ \AA}$; Δ full width half maximum (FWHM), and θ diffracting angle. Optical properties of the Bi doped TiO₂/kaolinite were investigated using UV-Visible diffuse reflectance spectrophotometry (DRS, Shimadzu 2450) with software UV Probe (DRS-8000 Shimadzu). Scans were performed over 200-800 nm and the band gap energy was determined using the tauch formula $(h\nu - E_g)^{1/n} = A(h\nu - E_g)$. The functional groups present in the samples were recorded with a FTIR analysis (Shimadzu IR Prastige21) over a wavenumber range of 400–4000 cm⁻¹.

2.5. Bacterial inactivation assessment

The bacterial inactivation activity of the Bi-TiO₂-K photocatalyst was evaluated under visible light irradiation conditions as described by Dedkova et al.[19]. Two different bacterial strains were used for the testing of antibacterial activity. The nutrient broth for the cultivation bacteria were used. Incubation of bacteria was conducted in thermostat for 24 hours at 200 rpm and 37 °C in a shaking incubator. Suspension of the Bi-TiO₂-K photocatalyst in growth media was diluted to achieve concentrations of 5.0 mg/ml in the growth media which is contained of the bacterial inoculums of E. coli (Gram negative) and S.aureus (Gram positive) an initial cell concentration of 1.3 \times 10⁸ CFU its equal to optical density (OD) 0.29 and 4 \times 10⁹ CFU OD 0.2 respectively. The bacterial cells were harvested by centrifugation at 4000 rpm for 10 min in phosphate-buffered solution (pH = 7.0). The inactivation assessment was conducted under dark and visible light with ($\lambda \geq 400 \text{ nm}$) irradiation using a lamp Light Emitting Diode (50 wat) which placed 15 cm above the reactor tube to induce photocatalytic reaction for 180 minutes. After the exposure, bacterial inactivation activity was measured by turbidimetric method by measuring optical density using UV-Vis spectrophotometer. The Optical Density (OD) was determined every 20 min at wavelength of 600 nm using a UV-Vis spectrophotometer method to monitor bacterial inactivation. The reduction in turbidity was evaluated as an indication of the reduced quantity of E. coli and S. aureus bacterial in solution medium.

3. RESULTS AND DISCUSSIONS

The XRD patterns of the TiO₂ and Bi-TiO₂ composites after calcined at 400; 500 and 600oC for 2 hours are shown in Fig.1

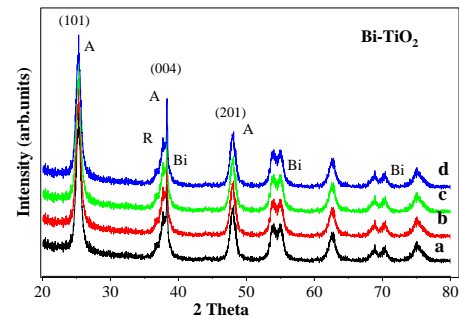


Figure 1 XRD pattern of the: a) TiO₂ and Bi-TiO₂ after calcined: b) 400; c) 500 and d) 600°C..

The diffraction peaks belonging to anatase are observable of the diffraction pattern after calcination at 400-500oC, which are indicated the fact that TiO₂ is present in the form of a pure crystalline phase. In the 600oC calcination treatment, the anatase phase was transformed into a rutile crystal phase [20]. Similar result was obtained with Xin et al. [21] where is anatase phase of 85% of the Bi-TiO₂ samples after calcined at 600°C. It is suggested that at least for calcined bellow 500°C the doping of Bi³⁺ cation into the TiO₂ lattice therefore does not give significant changes in the XRD pattern.

The FTIR spectra provided functional groups information about the prepared samples. Fig 2 shows a broad spectrum of Bi-TiO₂-K which is ascribe characteristic of kaolinite [19]. The presence of broad band at 3500 cm⁻¹ is ascribe to the vibrations of the O-H groups. The appearance of band at 450-550 cm⁻¹ represents the vibrational of Ti-O-Ti [6].

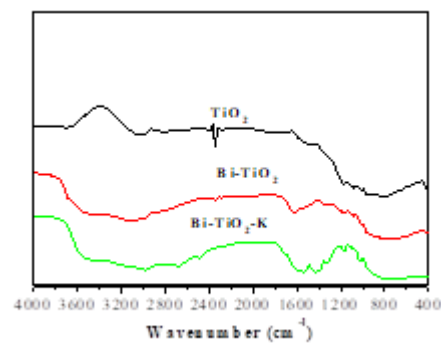


Figure 2 FTIR spectra of the: TiO₂, Bi-TiO₂ and Bi-TiO₂-K samples

The presence of broad band at 3500 cm⁻¹ is ascribed to the vibrations of the O-H groups. The appearance of band at 450-550 cm⁻¹ represents the vibrational of Ti-O-Ti [6]. Regarding the Bi-TiO₂ and Bi-TiO₂-K spectrum observed in the region of 800-850 cm⁻¹ this is attributable to stretching of the Bi-O [22]. This indicates that the Bi³⁺ cation was successfully incorporating in TiO₂ lattice sites. In addition is less information about Bi-TiO₂ due to its very broad bands of Bi-TiO₂-K.

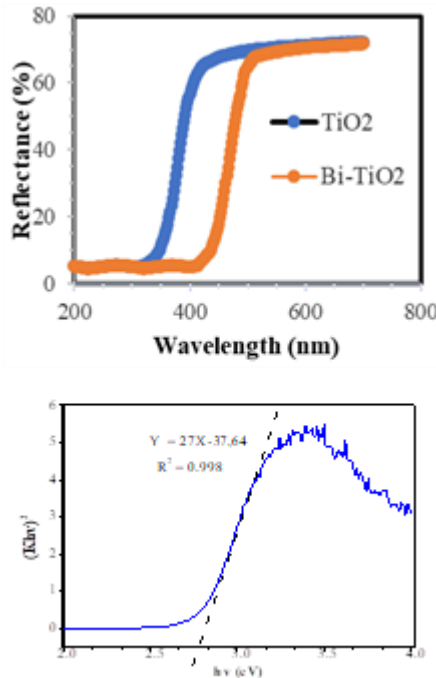


Figure 3 UV-vis DRS of a) pure TiO₂ and Bi-TiO₂ ; b) Tauch plot (K α h ν)² vs h ν of Bi-TiO₂

The reflectance (%R) properties of the prepared samples were examined using the UV-vis DRS method. Fig. 3 shows the corresponding UV-vis DRS of pure TiO₂, and Bi-TiO₂. The absorption edge of pure TiO₂ is below 400 nm due to the intrinsic inter-band transition absorption of anatase TiO₂. Compared with pure TiO₂, the respective optical absorptions of Bi-TiO₂ were enhanced to the visible light region. It indicates that the lattice defects and disorders introduced through the incorporation of the Bi³⁺ cations into TiO₂ lattice sites [20]. The band gap energy (E_g) of the photocatalysts was determined using Tauc equation [6], [23], [24].

$$(\alpha h\nu) = A(h\nu - E_g)^2 \tag{1}$$

where α is the absorption coefficient, A is a constant depending on electronic transitions and $h\nu$ is the photon energy. The band gap energy (E_g) was obtained by taking the intercept of the extrapolation of the linear region of the plot (k α h ν)² versus h ν (Fig. 3b). The band gap of the Bi-TiO₂ (2.76 eV) decrease from 3.22 eV (TiO₂) is caused by incorporating Bi³⁺ cation to form Bi-O-Ti bonds [10]. These results suggest that Bi-TiO₂ photocatalyst exhibit enhancement in photoresponse

under visible light. This red shift which occurred for Bi-TiO₂ was evidenced by its corresponding into consideration the spin exchange interaction sp-d between band electrons and localized d electrons of Ti⁴⁺ cations substituting by the Bi³⁺ ions [17], [25]. In addition, after Bi doping onto TiO₂ lattice sites, the obtained photocatalysts showed a significantly enhanced optical absorption extending to the visible-light region.

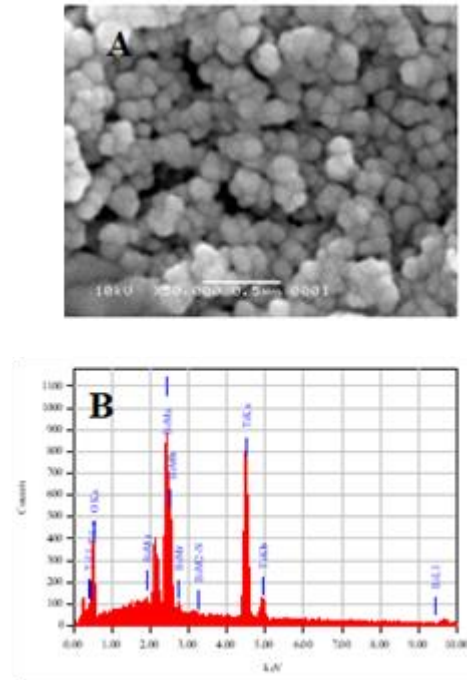


Figure 4 (A) SEM Image of Bi-TiO₂-K ; (B) EDX spectrum of Bi-TiO₂-K

Fig. 4 (A) provides a SEM image the prepared Bi-TiO₂-K photocatalyst. According to the SEM image, the Bi atoms are homogeneously dispersed on the surface of TiO₂ nanoparticles. One may understand that the prepared photocatalyst is composed of agglomerated high-density nanoparticles, which is expected to expand the photoresponse region, and increase the photo-carrier charge photoelectron (e⁻) and photohole (h⁺) transfer to the surface of the nanocomposite prior to their recombination. From the EDX spectrum Fig. 4(B), showed that the Bi-TiO₂ photocatalyst contains 3 elements, such as O, Ti, Bi and Si, with atomic ratio are 55.38; 33.04; 4.00 and 7.58 %, respectively. The bismuth content in the TiO₂ lattice indicates that the Bi³⁺ cations have been successfully incorporated into TiO₂ lattice. Substitution of some the Ti⁴⁺ by Bi³⁺ cations will reduce the photocatalyst band gap. This is consistent with the results of DRS spectra Bi-TiO₂ photocatalyst which has a band gap energy of 2.76 eV.

The effect of photocatalytic reaction of the TiO₂, Bi-TiO₂ and Bi-TiO₂-K photocatalyst on the growth of EC and SA under visible irradiation for 180 minutes are shown in Fig 5A and 5B respectively. Two control experiments containing only the photocatalyst under dark

(adsorption) and light conditions (photolysis) were conducted [26]. Photolysis and adsorption phenomenon showed non-significant inactivation EC and SA. These results imply that usage visible light in the absence of photocatalyst was incapable to inactivate EC and SA bacteria [27]. It can be seen in fig 5. The TiO₂ have a slight inactivation of EC and SA under visible light. In generally, the TiO₂ photocatalyst cannot be activated by visible light, because its band gap (eg) is high (3.0-3.2 eV). These results indicate that LED lamps as used as a visible light source still contain UV light at a portion of 10%. It can be seen in fig. 5A dan 5B the TiO₂ have a low photocatalytic bacterial inactivation.

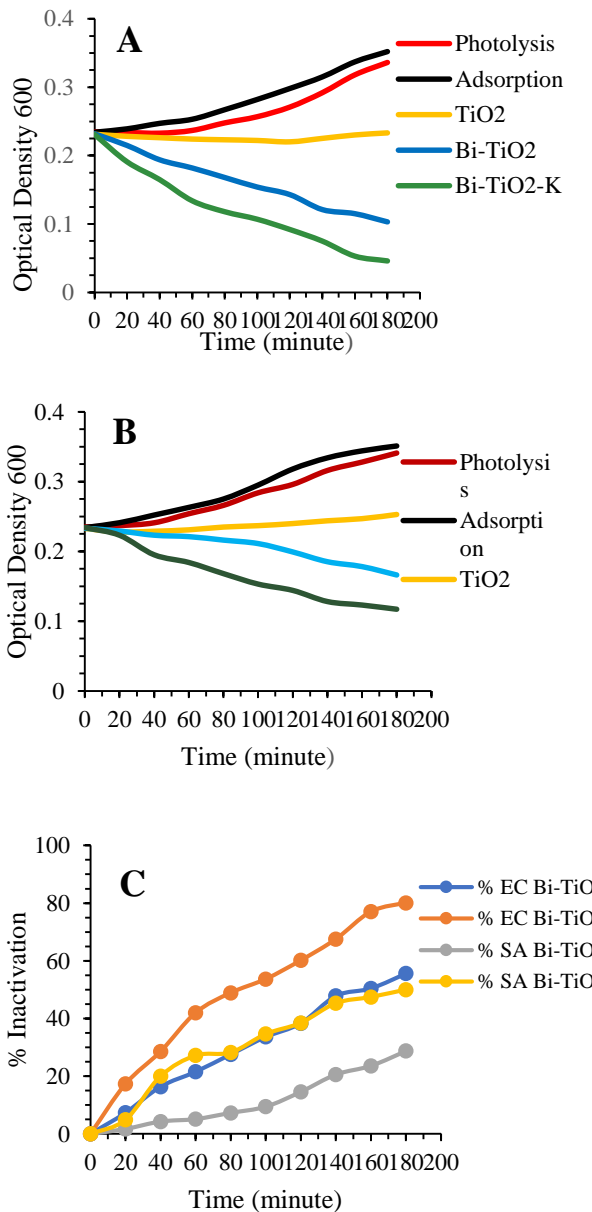


Figure 5 Growth curves: A) EC; B). SA bacteria on different processes, and (C) % Inactivation for E. coli (EC) and S.Aureus (SA)

The Bi-TiO₂ showed good inactivation for EC and SA bacteria under visible light irradiation. The optical

density (OD) 600 value for EC and SA bacterial using Bi-TiO₂ is much lower than TiO₂ after visible light irradiated for 180 min, where arise to 0.103; 0.166 and 0.253 respectively. These results are consistent with the band gap of TiO₂ decreases from 3.22 eV to 2.76 eV after Bi³⁺ is incorporated into the TiO₂ lattice site was observed in this study. It may be an indication that the formation of (e-) and (h+) pairs on the surface of Bi-TiO₂ photocatalyst is easier to occur than TiO₂ when absorbing visible light as a result of the mixing of the Bi 2p with Ti 2p orbitals [27], [28]. Obviously, the Bi³⁺ cation doping into TiO₂ lattice caused narrowed the band gap and improved the optical absorption visible light [11], [29].

In contrast, the photocatalytic inactivation for EC dan SA value showed superior of Bi-TiO₂/kaolinite photocatalyst under visible irradiation. It can be seen in fig 5.C that photocatalytic inactivation for EC using Bi-TiO₂/kaolinite higher than Bi-TiO₂ photocatalyst after exposed with visible irradiation for 180 min capable to inactivate of EC by 80% and 55.6% respectively. For SA bacteria % inactivation using Bi-TiO₂/kaolinite and Bi-TiO₂ photocatalyst after exposed with visible irradiation for 180 min was observed are 50% dan 28,75% respectively.

The immobilization of Bi on the kaolinite surface can expand the active site so that the adsorption capacity of bacterial substrates on the photocatalyst surface increases causing an increase in the number of inactive bacteria[19]. According to Manikandaan et al., enhancement photocatalytic inactivation bacterial under visible light in the presence of Bi-TiO₂/kaolinite photocatalysts could be explained by the high specific surface area of kaolinite was prepared [19] to provide additional active surface sites to adsorb water molecules and to form active radical hydroxide (OH•) [26]. There was improved the surface area of the photocatalyst caused enhance its capacity absorption. It was clearly that the higher inactivation of EC are simultaneously contribution of the high surface area of kaolinite as site active to substrate absorption. Another factor of the superoxide anion radicals (O₂^{-•}) and hydroxyl radicals (•OH) pairs are able to oxidize bacteria. Enhanced photocatalytic bacterial inactivation is a synergistic effect of doping Bi³⁺ on the optical properties and high surface area kaolinite on increase adsorption capacity of substrate bacteria.

The Bi-TiO₂/kaolinite photocatalyst showed more higher photocatalytic inactivation of EC bacteria than SA. One of the contributing factors is may affect antibacterial properties of nanoparticles is the fact that bacterial cells produce extracellular proteins. According to the cellular wall composition the bacteria are classified as Gram-positive and Gram-negative bacteria. The E. coli is a Gram-negative bacterial with the outer cell membrane covered by a lipopolysaccharide layer of 1-3

□m thickness [32]. E. coli is a gram-negative bacteria that gives a negative charge in the solution media, it will be stronger to interact with the positively charged TiO₂ surface, so that it is more easily adsorbed to the Bi-TiO₂-K surface compared to S.Aureus which is positively charged. With the slightly negatively charged outer E. coli surface, it is expected that this bacterium could have an enhanced photocatalytic inactivation rate with a Bi-TiO₂-K photocatalyst. This is owing to the nature of the heterogeneous TiO₂ photocatalytic reaction, where the bacterial contaminants transfer to the vicinity of the TiO₂ surface for subsequent cyclic radical hydroxyl penetration

4. CONCLUSION

The Bi-TiO₂-K photocatalyst have been fabricated. The band gap of the Bi-TiO₂ (2.76 eV) decrease from 3.22 eV (anatase TiO₂) was caused by incorporating Bi³⁺ cation to form Bi-O-Ti bonds caused responsive to visible light region. Immobilization of Bi-TiO₂ on the kaolinite surface increased the photocatalytic inactivating EC and SA bacteria after visible light irradiation for 180 min arise 80% and 50% inactivation EC and SA bacteria respectively.

ACKNOWLEDGMENT

Acknowledgments. This work was funded by the Kementerian Pendidikan, Kebudayaan, Riset & Teknologi, Universitas Tanjungpura, Republik Indonesia.

REFERENCES

- [1] H. J. Cui, H. Z. Huang, B. Yuan, and M. L. Fu, "Decolorization of RhB dye by manganese oxides: Effect of crystal type and solution pH," *Geochem. Trans.*, vol. 16, no. 1, pp. 10–12, 2015, doi: 10.1186/s12932-015-0024-2.
- [2] G. Li et al., "Enhanced visible-light-driven photocatalytic inactivation of Escherichia coli using g-C₃N₄/TiO₂ hybrid photocatalyst synthesized using a hydrothermal-calcination approach," *Water Res.*, vol. 86, pp. 17–24, 2015, doi: 10.1016/j.watres.2015.05.053.
- [3] S. Ma, S. Zhan, Y. Jia, and Q. Zhou, "Superior Antibacterial Activity of Fe₃O₄-TiO₂ Nanosheets under Solar Light," *ACS Appl. Mater. Interfaces*, vol. 7, no. 39, pp. 21875–21883, 2015, doi: 10.1021/acsami.5b06264.
- [4] D. A. Solís-Casados, L. Escobar-Alarcón, A. Arrieta-Castañeda, and E. Haro-Poniatowski, "Bismuth–titanium oxide nanopowders prepared by sol–gel method for photocatalytic applications," *Mater. Chem. Phys.*, vol. 172, no. February, pp. 11–19, Apr. 2016, doi: 10.1016/j.matchemphys.2015.12.002.
- [5] P. Kehrein, M. van Loosdrecht, P. Osseweijer, M. Garfi, J. Dewulf, and J. Posada, "A critical review of resource recovery from municipal wastewater treatment plants – market supply potentials, technologies and bottlenecks," *Environ. Sci. Water Res. Technol.*, vol. 6, no. 4, pp. 877–910, 2020, doi: 10.1039/C9EW00905A.
- [6] A. B. Aritonang, E. Pratiwi, W. Warsidah, S. I. Nurdiansyah, and R. Risko, "Fe-doped TiO₂/Kaolinite as an Antibacterial Photocatalyst under Visible Light Irradiation," *Bull. Chem. React. Eng. Catal.*, vol. 16, no. 2, pp. 293–301, 2021, doi: 10.9767/bcrec.16.2.10325.293-301.
- [7] A. B. Aritonang, Y. K. Krisnandi, and J. Gunlazuardi, "Modification of TiO₂ nanotube arrays with N doping and Ag decorating for enhanced visible light photoelectrocatalytic degradation of methylene blue," *Int. J. Adv. Sci. Eng. Inf. Technol.*, vol. 8, no. 1, pp. 234–241, 2018, doi: 10.18517/ijaseit.8.1.2342.
- [8] V. Caratto et al., "Atividade antibacteriana de tubos endotraqueais revestidos com dióxido de titânio padrão e dopados com nitrogênio: Um estudo in vitro," *Rev. Bras. Ter. Intensiva*, vol. 29, no. 1, pp. 55–62, 2017, doi: 10.5935/0103-507X.20170009.
- [9] P. A. K. Reddy, B. Srinivas, P. Kala, V. D. Kumari, and M. Subrahmanyam, "Preparation and characterization of Bi-doped TiO₂ and its solar photocatalytic activity for the degradation of isoproturon herbicide," *Mater. Res. Bull.*, vol. 46, no. 11, pp. 1766–1771, Nov. 2011, doi: 10.1016/j.materresbull.2011.08.006.
- [10] S. Murcia-López, M. C. Hidalgo, and J. A. Navío, "Synthesis, characterization and photocatalytic activity of Bi-doped TiO₂ photocatalysts under simulated solar irradiation," *Appl. Catal. A Gen.*, vol. 404, no. 1–2, pp. 59–67, 2011, doi: 10.1016/j.apcata.2011.07.008.
- [11] H. Mao, Z. Jin, F. Zhang, H. He, J. Chen, and Y. Qian, "A high efficiency photocatalyst based on porous Bi-doped TiO₂ composites," *Ceram. Int.*, vol. 44, no. 14, pp. 17535–17538, 2018, doi: 10.1016/j.ceramint.2018.06.074.
- [12] P. Magesan and A. Sviaraniyani, "Synthesis and Characterization of Bismuth Oxide Doped Titanium Dioxide and Its Antibacterial Activity," *Int. J. Pure Appl. Math.*, vol. 119, no. 12, pp. 6345–6359, 2018, [Online]. Available: <http://www.ijpam.eu>.
- [13] H. Li, J. Liu, J. Qian, Q. Li, and J. Yang, "Preparation of Bi-doped TiO₂ nanoparticles and their visible light photocatalytic performance," *Cuihua Xuebao/Chinese J. Catal.*, vol. 35, no. 9, pp.

- 1578–1589, 2014, doi: 10.1016/S1872-2067(14)60124-8.
- [14] N. V. S. Praneeth and S. Paria, “Clay-supported anisotropic Au-modified N,S-doped TiO₂ nanoparticles for enhanced photocatalytic dye degradation and esterification reactions,” *New J. Chem.*, vol. 44, no. 6, pp. 2619–2629, 2020, doi: 10.1039/c9nj05306a.
- [15] J. Ma, J. Chu, L. Qiang, and J. Xue, “Synthesis and structural characterization of novel visible photocatalyst Bi–TiO₂/SBA-15 and its photocatalytic performance,” *RSC Adv.*, vol. 2, no. 9, p. 3753, 2012, doi: 10.1039/c2ra01199a.
- [16] W. Zhou, P. Zhang, and W. Liu, “Anatase TiO₂ nanospindle/activated carbon (AC) composite photocatalysts with enhanced activity in removal of organic contaminant,” *Int. J. Photoenergy*, vol. 2012, pp. 28–30, 2012, doi: 10.1155/2012/325902.
- [17] V. L. Chandraboss, J. Kamalakkannan, and S. Senthilvelan, “Synthesis of activated charcoal supported Bi-doped TiO₂ nanocomposite under solar light irradiation for enhanced photocatalytic activity,” *Appl. Surf. Sci.*, vol. 387, pp. 944–956, 2016, doi: 10.1016/j.apsusc.2016.06.110.
- [18] T. H. da Silva et al., “Kaolinite/TiO₂/cobalt(II) tetracarboxymetallophthalocyanine nanocomposites as heterogeneous photocatalysts for decomposition of organic pollutants trimethoprim, caffeine and prometryn,” *J. Braz. Chem. Soc.*, vol. 30, no. 12, pp. 2610–2623, 2019, doi: 10.21577/0103-5053.20190178.
- [19] K. Dědková et al., “Antibacterial activity of kaolinite/nanoTiO₂ composites in relation to irradiation time,” *J. Photochem. Photobiol. B Biol.*, vol. 135, pp. 17–22, 2014, doi: 10.1016/j.jphotobiol.2014.04.004.
- [20] B. E. Nagay et al., “Visible-Light-Induced Photocatalytic and Antibacterial Activity of TiO₂ Codoped with Nitrogen and Bismuth: New Perspectives to Control Implant-Biofilm-Related Diseases,” *ACS Appl. Mater. Interfaces*, vol. 11, no. 20, pp. 18186–18202, 2019, doi: 10.1021/acscami.9b03311.
- [21] J. Xin, S. Zhang, and G. Qi, “PREPARATION AND CHARACTERIZATION OF THE Bi-DOPED TiO₂ PHOTOCATALYSTS Jian-Hua Xin, Shou-Min Zhang *, Guang-Dong Qi, Xiu-Cheng Zheng, Wei-Ping Huang and Shi-Hua Wu,” vol. 86, no. 2, pp. 291–298, 2005.
- [22] Y. Astuti, B. M. Listyani, L. Suyati, and A. Darmawan, “Bismuth oxide prepared by sol-gel method: Variation of physicochemical characteristics and photocatalytic activity due to difference in calcination temperature,” *Indones. J. Chem.*, vol. 21, no. 1, pp. 108–117, 2021, doi: 10.22146/ijc.53144.
- [23] A. El Mragui, Y. Logvina, L. Pinto da Silva, O. Zegaoui, and J. C. G. Esteves da Silva, “Synthesis of Fe- and Co-Doped TiO₂ with Improved Photocatalytic Activity Under Visible Irradiation Toward Carbamazepine Degradation,” *Materials (Basel)*, vol. 12, no. 23, p. 3874, Nov. 2019, doi: 10.3390/ma12233874.
- [24] M. A. M. Khan, S. Kumar, A. N. Alhazaa, and M. A. Al-Gawati, “Modifications in structural, morphological, optical and photocatalytic properties of ZnO:Mn nanoparticles by sol-gel protocol,” *Mater. Sci. Semicond. Process.*, vol. 87, pp. 134–141, Nov. 2018, doi: 10.1016/j.mssp.2018.07.016.
- [25] M. Salimi et al., “A new nano-photocatalyst based on Pt and Bi co-doped TiO₂ for efficient visible-light photo degradation of amoxicillin,” *New J. Chem.*, vol. 43, no. 3, pp. 1562–1568, 2019, doi: 10.1039/c8nj05020a.
- [26] V. Manikandan, M. A. Mahadik, I. S. Hwang, W. S. Chae, J. Ryu, and J. S. Jang, “Visible-Light-Active CuOx-Loaded Mo-BiVO₄ Photocatalyst for Inactivation of Harmful Bacteria (*Escherichia coli* and *Staphylococcus aureus*) and Degradation of Orange II Dye,” *ACS Omega*, vol. 6, no. 37, pp. 23901–23912, 2021, doi: 10.1021/acsomega.1c02879.
- [27] N. Khadgi, A. R. Upreti, and Y. Li, “Simultaneous bacterial inactivation and degradation of an emerging pollutant under visible light by ZnFe₂O₄ co-modified with Ag and rGO,” *RSC Adv.*, vol. 7, no. 43, pp. 27007–27016, 2017, doi: 10.1039/c7ra01782k.
- [28] D. A. Solís-Casados, L. Escobar-Alarcón, A. Arrieta-Castañeda, and E. Haro-Poniatowski, “Bismuth-titanium oxide nanopowders prepared by sol-gel method for photocatalytic applications,” *Mater. Chem. Phys.*, vol. 172, no. February, pp. 11–19, 2016, doi: 10.1016/j.matchemphys.2015.12.002.
- [29] B. Benalioua, M. Mansour, A. Bentouami, B. Boury, and E. H. Elandaloussi, “The layered double hydroxide route to Bi-Zn co-doped TiO₂ with high photocatalytic activity under visible light,” *J. Hazard. Mater.*, vol. 288, pp. 158–167, 2015, doi: 10.1016/j.jhazmat.2015.02.013.